ISSN 2393-8471

International Journal of Recent Research in Civil and Mechanical Engineering (IJRRCME)
Vol. 2, Issue 2, pp: (1-9), Month: October 2015 – March 2016, Available at: www.paperpublications.org

A Review of Shortcomings of driving principle for Spherical Drive Systems

[1]Ishwar Hebbar, [2]Shilpaj Bhalerao, [3]Soham Pendurkar, [4]Ketan Keskar, [5]Kaustub Kapadani

[1, 2,3,4,5] Department of Mechanical Engineering, P.E.S.M.C.O.E., Pune

Abstract: **Spherical drive system is a relatively new field of research, and it holds a lot of potential due to a ball's ability to be holonomic and rebound from collisions. In order to provide propulsion to such a completely closed sphere several methods have been put forward by different researchers. This article aims at putting together a definitive and complete list of the limitations of every propulsion system, so that future product designers and researchers may be able to decide on which propulsion system suits their purpose. This article will also help future researchers to identify and therefore find ways to overcome these limitations.**

Keywords: **Holonomic, Barycenter, COAM, OST.**

I. INTRODUCTION

Spherical drive is a promising area in future development in robotics, drive system, military and many other applications. Spherical drive has acquired a lot of fame due to their holonomic motion. A holonomic system is the one in which the orientation of the system doesn't affect the desired direction of motion. A spherical drive system can rebound from collision in a quick and non-destructive manner so it increases the safely of the drive.

The current research direction of spherical drive is heavily focused on internal mechanism and corresponding control systems. Due the fact that research efforts are sporadic and uncoordinated, researchers have yet to create an optimized and effective system [4].

Quintessential spherical drive would be truly holonomic without any friction loses and will be the most efficient system existing. There are many spherical systems which are classified on the basis of principle used in the system. These principles are Barycenter Offset (BCO), Conservation of Angular Momentum (COAM) and Outer Shell Transformation (OST). From the conclusion of research paper [1] we conclude that following are types of existing Spherical Systems.

Table 1: Table of Taxonomy: Type Number, Governing Principle, Source of Movement, and Dominant Power Factor.

Type	Principle	Method	Source of Movement	Power Factor	Example
1	BCO	Shifting COG	COG Shift	mdrive=mshell	R. Mukherjee et al. [6]
2	BCO	Single Wheel	Equilibrium Change	mdrive=mshell	Halme et al. [7]
3	BCO	Universal Wheel	Downward Force on Shell	$m_{drive}=m_{shell}$	Zhan et al. [8]
4	BCO	Pendulum	Torque about Diameter	$m_{bob}=m_{shell}$	Michaud et al. [9]
5	COAM	Single-Axis	Reaction force from spin of CMG	τx	Guanghui et al. [10]
6	CAOM	Triple-Axis	Precession Torque	$\tau x * \tau y$	Schroll et al. [11,12]
7	OST	Shell Transformation	Various	Various	Artusi, Wait, Yamanaka, Sugiyama et al. [13–16]

ISSN 2393-8471

International Journal of Recent Research in Civil and Mechanical Engineering (IJRRCME)
Vol. 2, Issue 2, pp: (1-9), Month: October 2015 – March 2016, Available at: www.paperpublications.org

This paper discusses the types of principles used to propel a spherical robot and their limitations. It will mostly focus upon the BCO principle, its further types and its shortcoming. It will also justify the lack of points in BCO principle.

II. GOVERNING PRINCIPLES FOR SPHERICAL DRIVES

Till date all the spherical drive systems work on 3 governing principles viz. BCO (Barycenter Shift Offset), COAM (Conservation Of Angular Momentum) and OST (Outer Shell Transformation). These principles are explained in paper [*Richard Chase and Abhilash Pandya, Review A Review of Active Mechanical Driving Principles of Spherical Robots, Robotics 2012, 1, 3-23; doi:10.3390/robotics1010003, 22 November 2012*] as

1. "Barycenter Shift Offset:

The term barycenter offset is used in spherical robots to describe the act of shifting a robot's center of mass (the barycenter) in order to produce a desired motion. Consider a robotic sphere resting in equilibrium. As its internal mechanisms move, the mass distribution of the ball will be shifted, causing the ball to roll to a new position of equilibrium. With proper timing and control methodologies, the robot can move smoothly through its environment. However, the main limitation of this method is that the maximum output torque is constrained because the center of gravity cannot be shifted outside of the shell. This can best be illustrated by picturing a pendulum inside a sphere, which is a common and straightforward design. A simplified two-dimensional model (See Figure 1) illustrates the torque that can be generated and mechanically applied to the outer shell. A weighted bob of a given mass swings on an armature about a support rod located through the center axis of the robot. As the bob rotates, the center of mass rotates accordingly and the robot rolls to equilibrium.

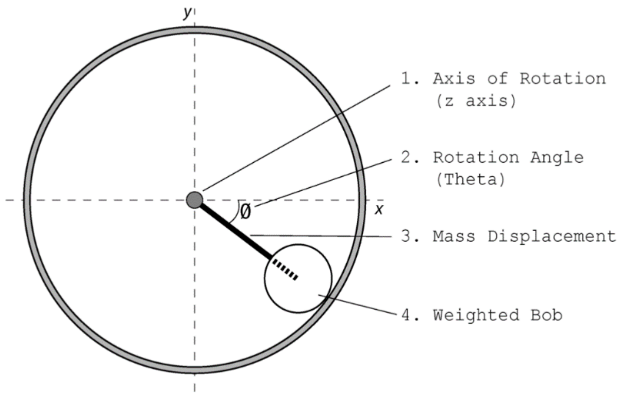

Fig.1: Cross section of a spherical robot model illustrating the pendulum drive armature and weighted bob.

The maximum value of the torque that can be applied is $\tau max = m\ g\ r * \sin(\theta)$ where τ is the output torque about the z-axis (Figure 1, item 1), mg is the weight of the bob (Figure 1, item 4), r is the displacement of the bob's center of mass from the shell's center of mass (Figure 1, item 3), and $\sin(\theta)$ corresponds to the rotation angle from the horizontal (Figure 1, item 2). What follows are variations of the barycenter offset designs."

BCO principle designs can be classified on the basis of frictional force involved in the system. Thus they can be classified as Frictional Barycenter Offset Drive and Non-frictional Barycenter Offset Drive. Frictional Barycenter Offset Drive system consists of frictional forces between the inner/outer surface of sphere and wheels used for controlling the drive.

- **Frictional Barycenter Offset Drive system:**

Sphere with Robot:

The early design of spherical drive consists of a robot placed inside a sphere. This robot were controlled by the remote controller. Whenever the robot moves, it shifts the barycenter of the sphere in the direction of the motion of the robot thus driving the sphere in same direction. Based on the design of the chassis of the robot, the motion of the sphere is decided. It can be made holonomic or non-holonomic depending upon the configuration of the wheels of the robot. Using Mecanum wheels or Omni-directional wheels, holonomic drive can be obtained while using simple wheels non-holo nomic drive can be obtained.

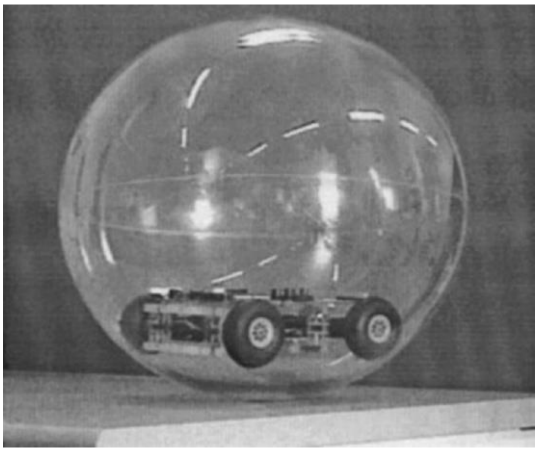

Fig.2: Prototype of a Hamster Ball design [5].

The drawback of this design is that if the friction coefficient between the wheels of robot and the inner surface of the sphere is not sufficient then it will lead to the slipping of the robot inside the sphere thus shifting the barycenter backwards and opposing the motion of the sphere. Another drawback is that due to the spherical shape, the torque of the drive is limited. Since the barycenter cannot be shift outside the sphere, torque of the system is limited. Due to the friction present in the system, power losses are induced in the system thus reducing the efficiency of the system.

Motion Model:

A basic motion analysis for the spherical robot can be easily performed using techniques similar to other _elds of robotics and explained in many textbooks, such as, for example, references [**11**] and [**12**]. In the following paragraphs, the kinematics of this device will be developed. Consider the contact point *c*=(*x*c , *y*c) between the spherical robot and the plane, as shown in Fig. 5. Assume that there are no slippages between the spherical shell and the plane of movement. This point *c* moves and describes a continuous trajectory in the plane when the spherical robot rolls. An inertial coordinate frame *{O}* is attached to the planar surface and another coordinate frame *{C}* is attached to the instantaneous contact point *a* between the sphere and the plane. In respect to coordinate frame *{O}*, the motion of coordinate frame *{C}* consists only of a linear motion along its *x* axis and a rotational motion around the *z* axis. Since the only component of velocity *v* in coordinate frame *{C}* is along the *x* axis, the motion equations on the plane can be written as

$$x_c(t) = x(0) + \int_0^t v(t)\cos(\alpha_1)dt \quad (1)$$

$$y_c(t) = y(0) + \int_0^t v(t)\sin(\alpha_1)dt \quad (2)$$

$$\alpha_1 = \alpha_1(0) + \int_0^t \omega_c(t)dt \quad (3)$$

Kinematical model:

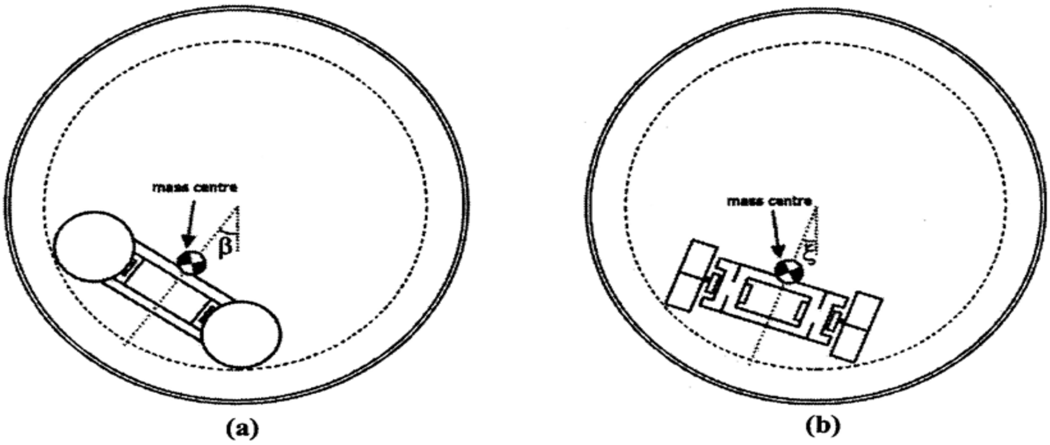

Fig.3: Motion model is equivalent to a pendulum: (a) side view, (b) front view

ISSN 2393-8471

International Journal of Recent Research in Civil and Mechanical Engineering (IJRRCME)
Vol. 2, Issue 2, pp: (1-9), Month: October 2015 – March 2016, Available at: www.paperpublications.org

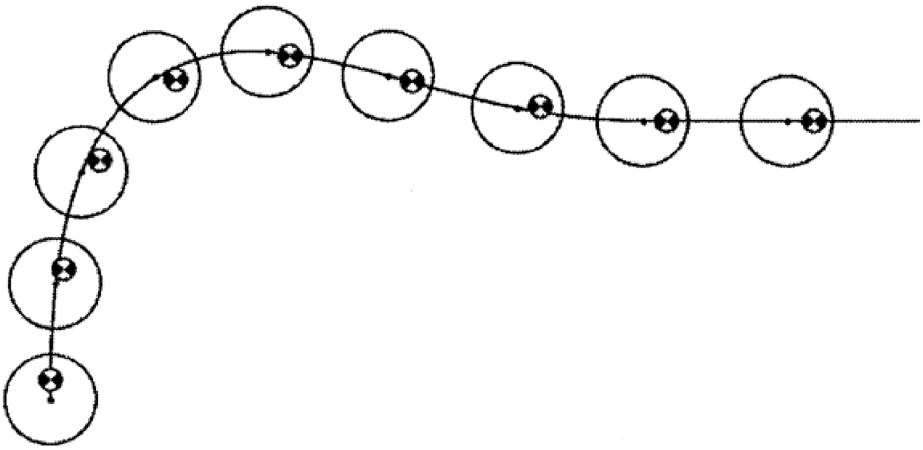

Fig.4: Centre of gravity of the robot projected on the ground. Robot steering is controlled based on the path curvature *k*(*t*)

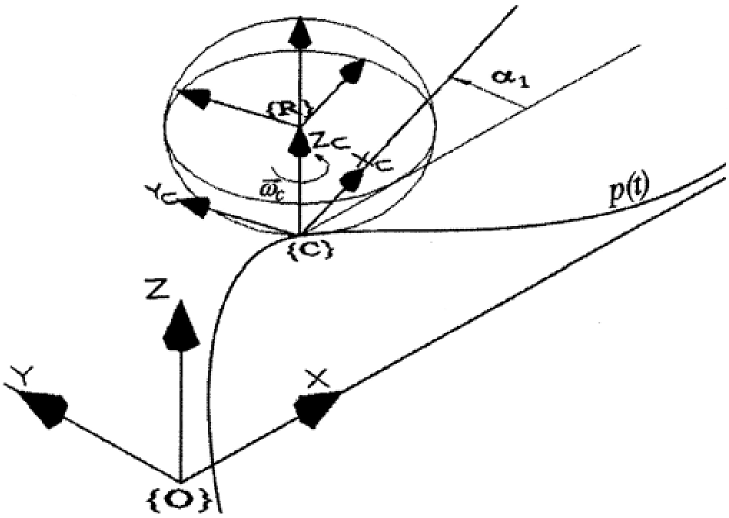

Fig.5: Motion on a plane

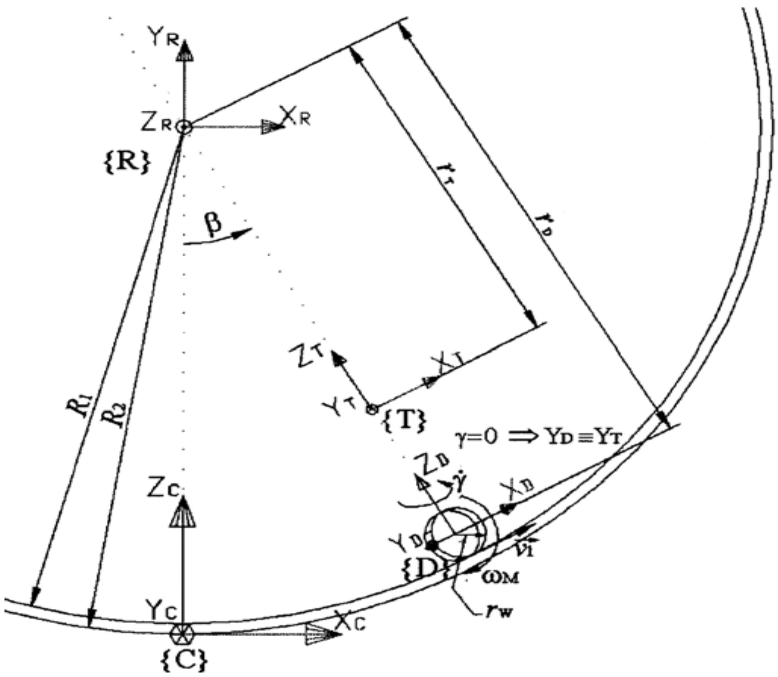

Fig.6: Motion inside the spherical robot

ISSN 2393-8471

International Journal of Recent Research in Civil and Mechanical Engineering (IJRRCME)
Vol. 2, Issue 2, pp: (1-9), Month: October 2015 – March 2016, Available at: www.paperpublications.org

Inside the spherical robot, consider the more general case of the internal unit being a single virtual wheel. This virtual wheel rests in a spherical shell with its internal radius equal to the radius of the circle described by the contact points between the internal unit's wheels and the inner spherical surface of the real robot. As seen in Fig. 6, a coordinate frame, *{R}*, is attached to the center of the sphere. Another coordinate frame, *{D}*, is attached to the center of the virtual wheel with the *x* axis having the wheel's orientation and the *y* axis being perpendicular to it. An auxiliary coordinate frame, *{T}*, is attached to the robot's mass center. The virtual wheel has radius r_W and rotates with an angular velocity $\boldsymbol{\omega_M}$ around the *y* axis of coordinate frame *{D}*. This angular velocity $\boldsymbol{\omega_M}$ translates into a linear velocity, v_1, for the contact point between the virtual wheel and the inner spherical surface. The virtual wheel also presents angular velocity $\dot{\gamma}$ around the *z* axis of coordinate frame *{D}* in order to reorient the direction of motion. The rotation speed of the wheel, with respect to coordinate frame *{D}*, is given by

$$^{D}\boldsymbol{\omega_M} = [\,\mathbf{0} \quad \frac{v_1}{r_w} \quad \mathbf{0}\,]^{T} \qquad \textbf{(4)}$$

Defining $^{R}\mathbf{R}_D$ as a rotation matrix that expresses the orientation of the referential *{D}* with respect to *{R}*, this rotation speed [equation (4)] can be expressed in coordinate frame *{R}* as

$$^{R}\boldsymbol{\omega_M} = {}^{R}\mathbf{R}_D\, {}^{D}\boldsymbol{\omega_M} = -\frac{v_1}{r_w}\begin{bmatrix} c_\beta\, s_\gamma \\ s_\beta\, s_\gamma \\ c_\gamma \end{bmatrix} \qquad \textbf{(5)}$$

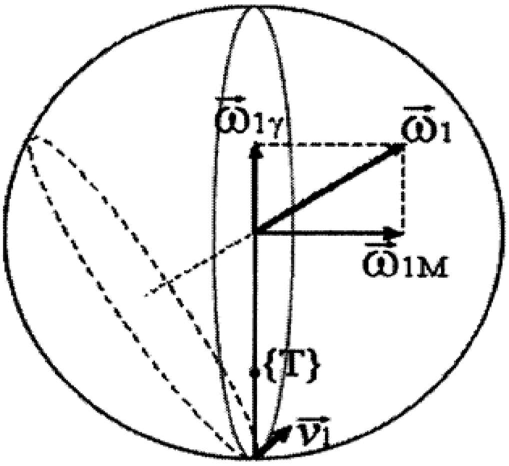

Fig.7: Representation of the internal unit's angular velocity

Where c_Θ and s_Θ are shorthand for cos (Θ) and sin (Θ) respectively The virtual wheel angular velocity $^{R}\boldsymbol{\omega_1}$can be decoupled on two velocities $^{R}\,\boldsymbol{\omega_1}_M$ and $R\boldsymbol{\omega_1}_\gamma$, resulting from velocities $\boldsymbol{\omega_M}$ and $\dot{\gamma}$ (see Fig. 6). As illustrated in Fig. 7, these two velocities are related by the equation:

$$^{R}\boldsymbol{\omega_1} = \; R\,\boldsymbol{\omega_1}_M + \; R\boldsymbol{\omega_1}_\gamma$$

From equation (5) and considering the total radius inside the sphere $(r_D + r_W)$, the velocity component $R\,\boldsymbol{\omega_1}_M$ is given by:

$$^{R}\,\boldsymbol{\omega_1}_M = \frac{r_W}{r_D + r_W}\,(-{}^{R}\boldsymbol{\omega_M})$$

$$= \frac{v_1}{r_D + r_W}\begin{bmatrix} c_\beta\, s_\gamma \\ s_\beta\, s_\gamma \\ c_\gamma \end{bmatrix} \qquad \textbf{(6)}$$

Which expresses its proportionality to $^{R}\boldsymbol{\omega_M}$**.** Defining $^{R}\mathbf{R}_T$ as a rotation matrix that expresses the orientation of the referential *{T}* with respect to the referential *{R}*,and expressing velocity $\dot{\gamma}$ as a vector, the component

$^{R}\,\boldsymbol{\omega_1}_\gamma$ is given by

$$^{R}\,\boldsymbol{\omega_1}_\gamma = {}^{R}R_T\,{}^{T}\dot{\gamma} = {}^{R}\mathbf{R}_T\begin{bmatrix} 0 \\ 0 \\ \dot{\gamma} \end{bmatrix}$$

$$= \begin{bmatrix} -\dot{\gamma} s_\beta \\ \dot{\gamma} c_\beta \\ 0 \end{bmatrix} \quad \textbf{(7)}$$

It should be noticed that only the two components of ${}^{R}\boldsymbol{\omega_1}$ along the *z* axis and the *y* axis are important for this modelling, which can be expressed by algebraic transformations

$$\dot{\beta} = ({}^{R}\boldsymbol{\omega_1})^{T} \begin{bmatrix} \mathbf{0} \\ \mathbf{0} \\ \mathbf{1} \end{bmatrix} = \frac{v_1\, c_\gamma}{r_D + r_W} \quad \textbf{(8)}$$

$$\dot{\alpha}_1 = ({}^{R}\boldsymbol{\omega_1})^{T} \begin{bmatrix} \mathbf{0} \\ \mathbf{0} \\ \mathbf{1} \end{bmatrix} = \frac{v_1 s_\beta\, s_\gamma}{r_D + r_W} + \dot{\gamma} c_\beta \quad \textbf{(9)}$$

The linear velocity of the robot is then expressed by

$$V = \dot{\beta} R_2 \quad \textbf{(10)}$$

Results from equations (8), (9) and (10) can be combined with equations (1), (2) and (3), giving the global kinematical model of the spherical robot.

Dynamic model:

The dynamic model is necessary to model the robot's behavior and to have a good knowledge of its motion properties. Since the robot has its own inertia, it will not respond instantly to velocity commands. Assume, without loss of generality, that the internal unit concentrates its mass *M* in a single point, which is the origin of referential *{T}* (see Fig. 8). Define a plane passing through the origins of the referential *{R}*, *{T}* and *{C}*. This plane will be used as the reference plane in order to develop the dynamic model below. To simplify the description referential names will be omitted. The unbalanced mass center translates into a torque given by the expression

$$\tau = \boldsymbol{d}_{CM} \times M\boldsymbol{g} \quad (11)$$

This torque causes an angular acceleration as given by :

$$\tau = I\, \alpha' \quad (12)$$

Combining equations (11) and (12), the angular acceleration α' can be expressed as a function of the angle θas

$$d_{CM}\, Mg \sin(\theta) = I\, \alpha' \quad (13)$$

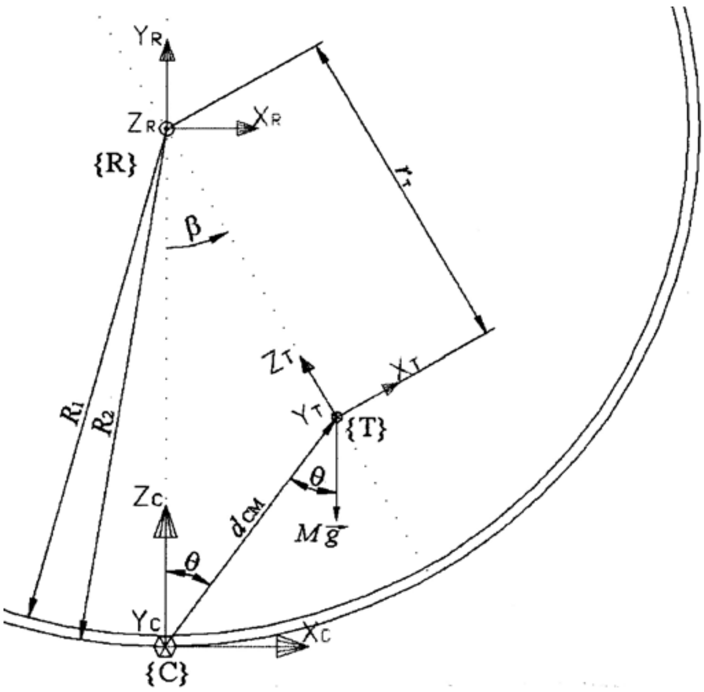

Fig.8: Effect of moving the internal unit

Since s_θ *and* s_β are related by trigonometric relations

$$\frac{r_T}{s_\theta} = \frac{d_{CM}}{s_\beta} = s_\theta = \frac{s_\beta \, r_T}{d_{CM}} \qquad (14)$$

Since angle b is easier to obtain from sensory data, expression (13) is rewritten as a function of b instead of Ɵ:

$$r_T \, M \, g \, s_\beta = I \, \alpha' \qquad (15)$$

Examples of Frictional Barycenter Offset Drive system are Hamster Ball [1], Internal Drive Unit (IDU) [1] and Universal Wheel [1]

- **Non-Frictional Barycenter Offset Drive system:**

Pendulum Driven Spherical Drive System [1]

To overcome the drawbacks of the frictional systems, non-frictional drive system were invented. This systems consists of the bob rotating about an axis of the sphere. This bob is suspended on the axis of sphere thus acting like pendulum of the clock. When this bob is rotated about the axis, the barycenter of the sphere is shifted thus resulting in the motion of the sphere. In this system, since there is no contact between the bob and the inner surface of the sphere, frictional forces are not involved thus reducing the power losses and increasing the efficiency of the system. Using further developed mechanism, the sphere can be steered as in case of Rosphere. [17]

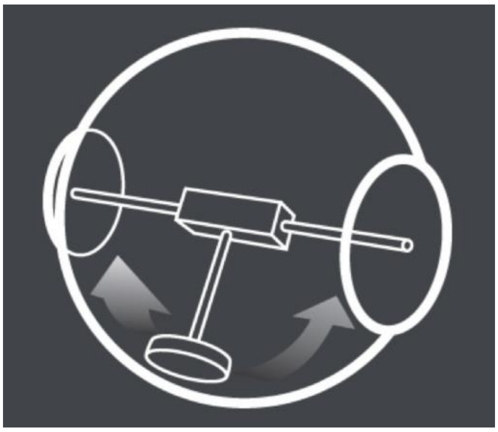

Fig.9: A commercialized pendulum-driven robot. Rotundus [3].

As the mass increases, the amount of torque that can be used to drive the sphere also increases. The most notable setback to this design is its inability to go up a steep slope. If the bob is where the majority of the weight of the system is located, the robot can go up a steep slope. However, in practice, a well-designed spherical robot can usually only go up about a 30° slope [11]. Rotundus can roll at speeds of 6mph, through snow, ice, mud, and sand, and can float. In addition, it can carry a 1.81 kg payload [3].

One drawback to this design is that the movement of the shell is non-holonomic: there is a turning radius associated with its movement.

Other examples of Non-Frictional Barycenter Offset Drive system are Double Pendulum [1].

The other principles of drive system as explained in paper (*Richard Chase and Abhilash Pandya, Review A Review of Active Mechanical Driving Principles of Spherical Robots, Robotics 2012, 1, 3-23; doi:10.3390/robotics1010003, 22 November 2012)* are as :

2. "Conservation of Angular Momentum (COAM) [1]

Barycenter offset designs are by far the most widely used design due to their lack of complication and ease of control, with shell transformation the next most frequent design. Although barycenter offset designs are commonly implemented, a major limitation is that because the center of mass can never go outside of the sphere, it becomes a torque-limited system.

In the last 20 years, the concept of adding control moment gyroscopes (CMGs) to a spherical robot has started to be investigated by various research groups. By spinning a large flywheel rapidly and rotating it about an axis, the laws of conservation of angular momentum can be used to control the movement of the sphere. Using this method relates the output torque of the internal mechanism to the angular velocity of the CMGs. As the angular velocity of the CMGs increase, so does the output torque. This is the most recent method in obtaining an output torque greater than that can be produced by a barycenter offset type system. To date, there have been multiple designs incorporating flywheels, each with varying successes and failures.

A unique feature of using a CMG is that these systems have reaction forces in all three spatial dimensions. If a CMG is spinning about the X-axis, and is rotated about the Y-axis, then there will be a torque about the Z-axis (precession). This feature has an obvious useful potential (generating a torque in the intended direction) but also causes control issues. Depending on the design of the robot, the precession torque can be utilized to control or augment the robot's angular momentum. However, if the design does not take this extra dimension of torque into account, it may steer the robot in an unwanted direction. Therefore, although a gyro-based or gyro-augmented spherical robot may be able to outpower—in terms of torque—a barycenter offset robot, there are other design challenges that must be faced before that can occur.

3. Outer Shell Transformation (OST) [1]

Although not as common as barycenter offset designs, shell transformation is also a novel method of propelling a spherical robot. This idea is fairly new and has some interesting concepts associated with it. Instead of a complicated internal mechatronics system to propel the sphere, the robot relies on transformation of its outer body. This can be achieved by deformation of the encompassing shell, or having environmental elements, such as wind or water, act on the body itself. Depending on the design, this family of robots may prove to be more versatile than a barycenter offset type of system. However, this concept is still in its infancy compared with the designs discussed above and it has potential for future research."

III. CONCLUSION AND DISCUSSION

The shortcomings of the Frictional BCO Drive system are as:

- Limited Torque: Due to the limitation, that the center of mass cannot be shifted outside the sphere, the torque of the system is limited to m g r*sin (θ).
- Frictional force between the inner surface of the sphere and the wheels (as in case of Hamster ball) or the bob reduces the efficiency of the system.
- Slipping between the inner surface of the sphere and wheel or bob makes the system unstable and difficult to control.
- Due to limited torque, the system cannot go up on steep slopes.
- The drive system is not holonomic so orientation adjustment is necessary.

Except frictional and slipping problems, all the shortcomings of the Non-Frictional BCO Drive system are same as Frictional BCO Drive system.

The shortcomings of the COAM Drive system are as:

- While using COAM, a gyroscopic couple acts on the system due to which controlling of the robot becomes very difficult.
- The system is not able to provide continuous torque.

The shortcomings of the OST Drive system are as:

The dead mass of the system becomes higher i.e. the weight of the mechanisms not currently being used is greater than the weight of the mechanism being used due to which the efficiency of the system decreases.

Thus we conclude that, there is no spherical drive design, till date, which uses Barycenter shift method and is frictionless and Holonomic. If such a design is created, then it will increase the efficiency of the drive and will have a number of applications. It will overcome the slipping problem, friction losses and thus the power utilization would increase. Such a design can revolutionize the existing spherical drive system.

REFERENCES

[1] Richard Chase and Abhilash Pandya, Review A Review of Active Mechanical Driving Principles of Spherical Robots, Robotics 2012, 1, 3-23; doi:10.3390/robotics1010003, 22 November 2012

[2] Alves, J.; Dias, J. Design and control of a spherical mobile robot. Proc IME J. Syst. Contr. Eng. 2003, 217, 457–467.

[3] Rotundus. Available online: http://www.rotundus.se (accessed on 22 May 2012).

[4] Liu, D.; Sun, H.; Jia, Q. A Family of Spherical Mobile Robot: Driving Ahead Motion Control by Feedback Linearization. In Proceedings of the 2nd International Symposium on Systems and Control in Aerospace and Astronautics (ISSCAA 2008), Shenzhen, China, December 2008;pp. 1–6.

[5] Alves, J.; Dias, J. Design and control of a spherical mobile robot. Proc IME J. Syst. Contr. Eng. 2003, 217, 457–467.

[6] Mukherjee, R.; Minor, M.; Pukrushpan, J. Simple Motion Planning Strategies for Spherobot: A Spherical Mobile Robot. In Proceedings of the 38th IEEE Conference on Decision and Control, Phoenix, AZ, USA, December 1999; Volume 3, pp. 2132–2137.

[7] Halme, A.; Schonberg, T.; Wang, Y. Motion Control of a Spherical Mobile Robot. In Proceedings of the 4th International Workshop on Advanced Motion Control (AMC'96-MIE), Tsu-City, Japan, March 1996; Volume 1, pp. 259–264.

[8] Zhan, Q.; Cai, Y.; Yan, C. Design, Analysis and Experiments of an Omni-Directional Spherical Robot. In Proceedings of 2011 IEEE International Conference on Robotics and Automation (ICRA), Shanghai, China, May 2011; pp. 4921–4926.

[9] Michaud, F.; Caron, S. Roball, the rolling robot. Auton. Robots 2002, 12, 211–222.

[10] Shu, G.; Zhan, Q.; Cai, Y. Motion Control of Spherical Robot Based on Conservation of Aangular Momentum. In Proceedings of International Conference on Mechatronics and Automation (ICMA 2009), Changchun, China, August 2009; pp. 599–604.

[11] Schroll, G. Dynamic Model of a Spherical Robot from First Principles. M.S. Thesis, Colorado State University, Fort Collins, CO, USA, 2010.

[12] Schroll, G. Angular Momentum Torque Enhancement for Spherical Vehicles. WO Patent WO/2010/057129, May 2010.

[13] Artusi, M.; Potz, M.; Aristizabal, J.; Menon, C.; Cocuzza, S.; Debei, S. Electroactive elastomeric actuators for the implementation of a deformable spherical rover. IEEE/ASME Trans. Mechatron. 2011, 16, 50–57.

[14] Wait, K.; Jackson, P.; Smoot, L. Self Locomotion of a Spherical Rolling Robot Using a Novel Deformable Pneumatic Method. In Proceedings of 2010 IEEE International Conference on Robotics and Automation (ICRA), Anchorage, AK, USA, May 2010; pp. 3757–3762.

[15] Yamanaka, T.; Nakaura, S.; Sampei, M. Hopping Motion Analysis of "Superball"-Like Spherical Robot Based on Feedback Control. In Proceedings of 2003 IEEE/RSJ International Conference on Intelligent Robots and Systems (IROS 2003), Las Vegas, NV, USA , October 2003, Volume 4, pp. 3805–3810.

[16] Sugiyama, Y.; Shiotsu, A.; Yamanaka, M.; Hirai, S. Circular/Spherical Robots for Crawling and Jumping. In Proceedings of 2005 IEEE International Conference on Robotics and Automation (ICRA 2005), Barcelona, Spain, April 2005; pp. 3595–3600.

[17] http://www.upm.es/internacional/UPM/UPM_Channel/News/9ec27b9df516f310VgnVCM10000009c7648aRCRD